Synthesis and Characterization of Colloidal InP Quantum Rods

ARTICLE *in* NANO LETTERS · MAY 2003

Impact Factor: 13.59 · DOI: 10.1021/nl034152e

NANO LETTERS

2003
Vol. 3, No. 6
833−837

Synthesis and Characterization of Colloidal InP Quantum Rods

S. P. Ahrenkiel,* O. I. Mićić, A. Miedaner, C. J. Curtis, J. M. Nedeljković, and A. J. Nozik

National Renewable Energy Laboratory, 1617 Cole Boulevard, Golden, Colorado 80401

Received March 11, 2003; Revised Manuscript Received April 17, 2003

ABSTRACT

InP nanorods and nanowires in the diameter range of 30–300 Å and 100–1000 Å in length were synthesized. For the preparation of nanorods, we used an organometallic precursor that decomposes thermally into InP and In metal particles. The latter serves as a nucleation catalyst for the growth of the semiconductor. Quantum rods of zinc blende structure with a high degree of crystallinity are grown along the (111) crystallographic planes. The absorption spectrum of InP nanorods with diameter of about 30 Å and 100–300 Å in length is in the visible spectral regime, suggesting a substantial blue shift with respect to the bulk (band gap 1.35 eV) that is due to size confinement. Moreover, the Stokes shift of the emission band in the quantum rods is substantially larger than the shift in the corresponding quantum dots.

1. Introduction. Over the past several years, considerable advances have been made toward the synthesis of colloidal semiconductor nanorods and nanowires with diameters sufficiently small to produce a quantum confinement of charge carriers. Notable progress has been made in the fabrication of crystalline III−V semiconductor fibers using laser-assisted growth,[1] template growth from carbon nanotubes,[2,3] and solution−liquid−solid reactions.[4] However, for these III−V semiconductors, these methods typically produce wires, hundred to thousands of angstroms in diameter and several micrometers in length, that are too large for the observation of size quantization effects. However, quantum rods of II−VI semiconductors have been synthesized with diameters of only 25−60 Å—well into the quantization regime—by controlling the difference in the growth rate among various crystallographic faces[5] or by self-assembly from oriented, individual quantum dots.[6]

The electrical and optical properties of semiconductor nanowires and nanorods are controlled by their diameter and shape. When the nanowire diameter is reduced such that quantum effects emerge, the optical band gap increases, and the absorption coefficient is enhanced at discrete wavelengths compared to those of the bulk material.[7] Quantum rods may also exhibit decreased Auger recombination rates compared to those of quantum dots,[8,9] which makes them potentially useful for quantum-rod lasers. The ability to prepare samples of smaller diameter and greater length allows the fundamental study of 1-D materials. The nanorod geometry also provides a preferred path for charge transport along the nanorod axis; thus, when organized into arrays of aligned quantum rods, improved electronic transport can be achieved compared to that of self-assembled 0-D quantum dots.[10]

Nanocrystalline InP fibers with diameters of hundreds of nanometers can be grown by a solution−liquid−solid mechanism at low temperature (111−203 °C), as described by Buhro and co-workers.[4,11] In their work, thermal decomposition of an organometallic precursor produces metal indium particles that catalyze the growth of the InP fibers. A similar mechanism has also been used to produce InP nanorods from solutions of indium salts, phosphorus, and a strong reducing agent at temperatures of 80−160 °C[12] or by a catalytic reaction from a hydrolyzed product of $[(Me)_2InP(SiMe_3)_2]_2$ onto indium particles at room temperature.[13] These approaches are analogous to the well-known, laser-assisted catalytic physical growth method, generally performed at higher temperatures (500 °C-1100 °C), in which metal particles are used to catalyze the growth of the semiconductor nanorod materials.[14,15]

In this communication, we demonstrate the formation of InP nanorods with diameters small enough to produce quantization effects. The optical properties of such InP nanorods are compared to those of InP quantum dots.

2. Experimental Section. *Preparation of InP Nanorods.* Synthesis was conducted in rigorously air- and water-free conditions following the standard Schlenk line technique. In(*t*-But)$_3$ and In(*t*-But)$_2$Cl were synthesized using established methods.[16] $[(t\text{-Bu})_2InP(SiMe_3)_2]_2$ was prepared from equimolar quantities of $(t\text{-Bu})_3In$ with $HP(SiMe_3)_2$ or $(t\text{-But})_2InCl$ with $P(SiMe_3)_3$. Colloidal InP nanorods were grown in 2% DDA (dodecylamine) in TOA (trioctylamine) or 2% TOPO (trioctyl phosphine oxide) in a TOP (trioctyl phosphine)

* Corresponding author. E-mail: phil_ahrenkiel@nrel.gov.

10.1021/nl034152e CCC: $25.00
Published on Web 05/13/2003

solution of 50 mg of In(*t*-But)$_2$Cl and 100 mg of $InCl_3$. In this solution, 350 mg of P(SiMe$_3$)$_3$ was added within a glovebox. Methanol (0.1 mL) was added to hydrolyze the P−SiMe$_3$ bond. This solution was stirred for 1 day. Next, the solution was heated in a Schlenk tube to 120, 170, and 250 °C for different time intervals and under rigorously air-free conditions. The solution containing the InP product turned brown after some time, and at higher temperature, a brown precipitate was formed. The resulting mixture was cooled, oxygen-free methanol was added, and the final product was washed.

The longer InP nanorods only partially dissolved in either chloroform or pyridine. Nanorods with diameters less than about 50 Å and lengths of a few hundred angstroms formed transparent solutions. The nanorods are extremely sensitive to oxygen and easily form an oxide layer at the surface with decreasing particle size. After synthesis, the nanorods contain impurities such as metallic In and various other byproducts. To clean the samples, they were washed carefully with methanol containing 0.5% HF that slightly etched the nanorod surface, removed impurities, and dissolved In^0 to form InF_3. Any remaining metallic In in the samples was removed by the addition of Hg droplets that extract the In metal by forming an alloy.

Optical Characterization. Optical absorption spectra were collected at room temperature using a Cary 5E UV−vis−NIR spectrophotometer. Photoluminescence spectra were obtained at room temperature using an SPEX Fluorolog-2 spectrometer.

Structural Characterization. Colloidal samples were deposited on C-coated Cu grids for microstructural analysis. Characterization was carried out on a Philips CM30 TEM operated at 200 kV. Bright-field and lattice images were acquired with an objective aperture that admitted contributions from low-index reflections. Selected-area patterns were acquired with an aperture having a projected diameter of approximately 7 μm in the image plane. EDX spectra were acquired with a Kevex Li-drifted Si detector using Emispec ESVision software. X-ray diffraction patterns were acquired on a Scintag $\times 1$ diffractomter using Cu Kα radiation.

After this paper was submitted for publication, a paper by Banin et al. appeared[17] on the formation of InAs quantum rods (diameter 40 Å, length 94−220 Å) using gold particles as the catalyst. This procedure yields InAs quantum rods with excellent quality and crystallinity. Although this method can also be applied to the synthesis of InP quantum rods,[17] it requires extremely small gold particles that are about 20 Å in diameter in order to lower the melting point of the gold particles to about 360 °C and initiate catalytic action. Indium has a lower melting point than gold, and the method described in this paper has the potential for greater flexibility for the synthesis of quantum rods with different diameters; it also allows for the chemical removal of the metallic indium catalyst from the rods. This is desirable because the presence of residual metal catalyst interferes with measurements of the electronic and optical properties of the quantum rods.

3. Results and Discussion. The growth of InP quantum rods and quantum wires by the solution−liquid−solid mechanism requires the presence of extremely small metal indium particles that serve as a catalyst for the growth of InP. The diameter of the indium particles determines the diameter of the nanorods. Indium particles can be introduced into the system before InP synthesis or can be produced simultaneously during InP growth from an organometallic molecular precursor by thermal decomposition. For the preparation of InP quantum rods, we used a mixture of [(*t*-Bu)$_2$InP(SiMe$_3$)$_2$]$_2$ and [Cl$_2$InP(SiMe$_3$)$_2$]$_2$ precursors. When only the [(*t*-Bu)$_2$InP(SiMe$_3$)$_2$]$_2$ precursor was present in the system, a large number of indium droplets and short InP fibers were produced. The [Cl$_2$InP(SiMe$_3$)$_2$]$_2$ precursor decomposes to InP without the formation of metallic indium and can produce InP fibers in the presence of metal indium particles.[18] Because of that, we added [Cl$_2$InP(SiMe$_3$)$_2$]$_2$ to [(*t*-Bu)$_2$InP(SiMe$_3$)$_2$]$_2$ to increase the total InP precursor concentration and, consequently, the length of the InP nanorods. Thermal decomposition of the [(*t*-Bu)$_2$InP-(SiMe$_3$)$_2$]$_2$ precursor is more suitable for the formation of extremely small quantum rods with diameters less than 60 Å because extremely small monodispersed metal indium particles are difficult to prepare. No metal indium particles or InP rods having diameters less than 60 Å have been reported previously in the literature.

The [(*t*-Bu)$_2$InP(SiMe$_3$)$_2$]$_2$ precursor has been used previously for the preparation of InP whiskers in toluene.[4] The main differences between our synthesis and this work[4] is that we used two precursors, [Cl$_2$InP(SiMe$_3$)$_2$]$_2$ and [(*t*-Bu)$_2$InP(SiMe$_3$)$_2$]$_2$, instead of only [(*t*-Bu)$_2$InP(SiMe$_3$)$_2$]$_2$ and that a strong stabilizer was in the solution in order to grow quantum rods. The diameter of the nanorods is very sensitive to the nature of the stabilizer present in solution. The TOA/DDA (trioctylamine/dodecylamine) stabilizer has the ability to coordinate In atoms strongly and thus to reduce the size of the indium metal particles drastically.[19,20] The alkylamine stabilizer TOA/DDA produces nanorods with smaller diameters than those produced by the conventional TOPO/TOP (trioctyl phosphine/trioctyl phosphine oxide) stabilizer. Figure 1 shows TEM images of InP nanorods of various dimensions. The structure and composition of the InP nanorods have been characterized using transmission electron microscopy (TEM) and energy-dispersive X-ray spectroscopy. Very small rods with diameters of 28 ± 7 Å (a) were prepared in TOA/DDA upon heating at 250 °C for 3 h, and larger wires with diameters of 50 Å to several hundred angstroms were prepared in TOPO/TOP upon heating at 250 °C for 30 min (b) and 24 h (c, d). All of these nanorods are much smaller in diameter than those previously prepared by thermal decomposition in toluene, a noncoordinating solvent.[4]

The range of rod diameters is evident in Figure 1. Rods with diameters from tens to a few hundred angstroms and lengths of up to several micrometers show strong crystallinity. As in other nanorod systems, (111) lattice fringes are resolved normal to the nanowire axis, with the corresponding [111] direction oriented parallel to the rod axis. Crystallographic analysis of the larger InP fibers is relatively straightforward. Inspection of a [110] zone (i.e., normal to

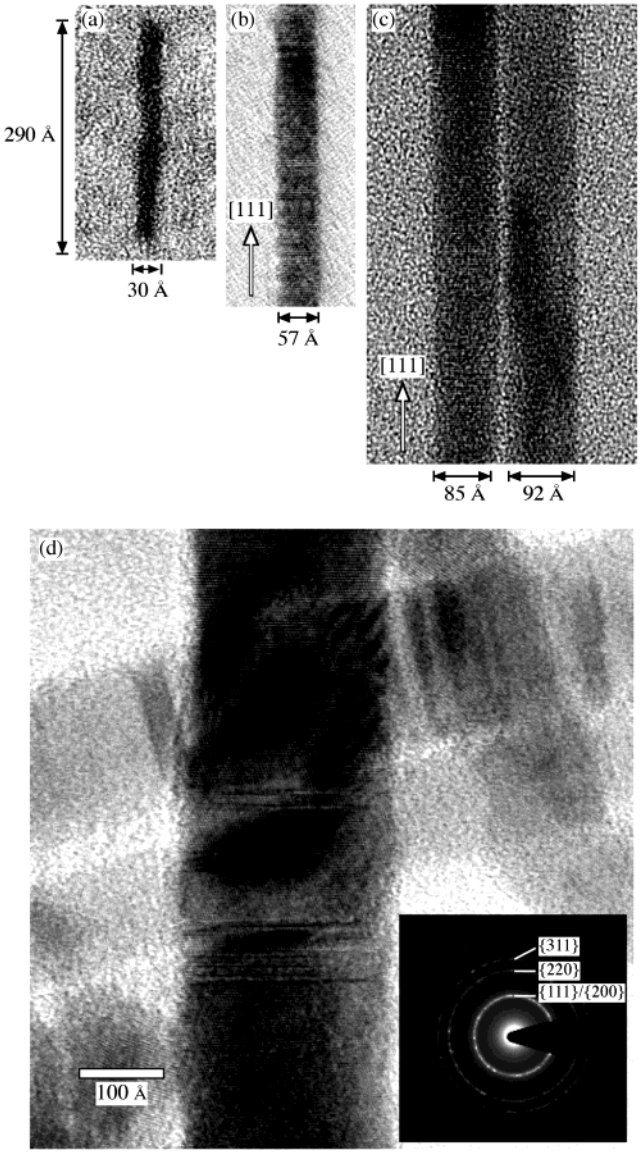

Figure 1. TEM images showing InP nanorods of various dimensions prepared in amine: (a) $[(t\text{-Bu})_2\text{InP}(\text{SiMe}_3)_2]_2$ and $[\text{Cl}_2\text{InP}(\text{SiMe}_3)_2]_2$ precursors in TOA/DDA heated at 250 °C for 3 h. The crystallinity of these very small nanorods is weak. (b, c) Prepared with $[\text{Cl}_2\text{InP}(\text{SiMe}_3)_2]_2$ precursor (without $[(t\text{-Bu})_2\text{InP}(\text{SiMe}_3)_2]_2$) on indium particles (diameter 60−110 Å) in TOA/ethylenediamine (0.1%) at 110 °C for 3 h. (d) $[(t\text{-Bu})_2\text{InP}(\text{SiMe}_3)_2]_2$ and $[\text{Cl}_2\text{InP}(\text{SiMe}_3)_2]_2$ precursors in TOP/TOPO heated at 250 °C for 24 h. The diameter distribution is broad (150−350 Å).

the wire axis) (Figure 1d) typically reveals (111) planar defects such as crystallographic twin boundaries or stacking faults.[16] These primarily constitute stacking disorder parallel to the growth direction and also arise to a lesser extent on oblique sets of (111) planes. Planar defects are a common occurrence in growth on {111} faces of close-packed compounds. Strong crystallinity can be maintained in fibers with diameters as small as 50 Å. Selected-area diffraction patterns from ensembles of the larger fibers show sharp, strong rings at positions consistent with the powder pattern for cubic InP. X-ray diffraction patterns show the presence of both cubic InP and tetragonal indium metal (Figure 2). Using the diffraction line widths, we obtain particle sizes of

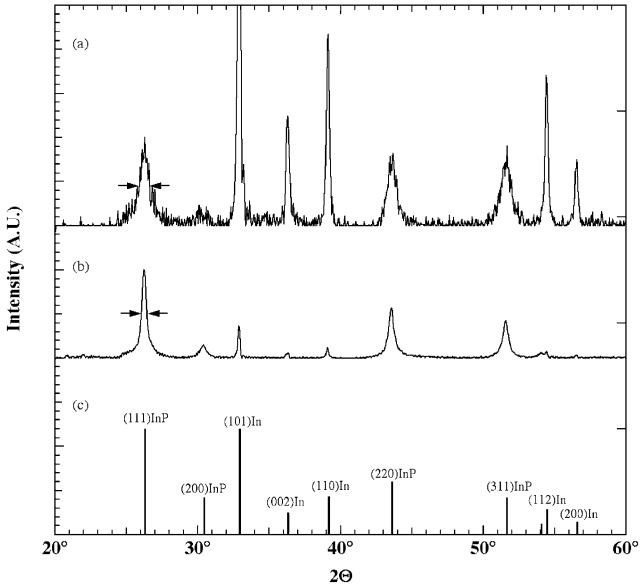

Figure 2. X-ray diffraction patterns from two ensembles of InP nanorods prepared with (a) $[\text{Cl}_2\text{InP}(\text{SiMe}_3)_2]_2$ on indium particles in TOA/ethylenediamine and (b) $[(t\text{-Bu})_2\text{InP}(\text{SiMe}_3)_2]_2$ and $[\text{Cl}_2\text{InP}(\text{SiMe}_3)_2]_2$ in TOP/TOPO. The pattern intensities were normalized to the (111) InP peaks. The arrows indicate the fwhm of the (111) InP peaks. (c) Powder diffraction lines for zinc blende InP and tetragonal indium.

typically 100−250 Å for the InP rods. (The particle sizes measured for the In metal are somewhat larger than those of the InP rods.)

We found that the nature of the stabilizers does not affect a crystallographic phase transformation from the zinc blende to wurtzite structure as was recently shown for GaP by Cohen et al.[21] Both InP and GaP semiconductors have a large difference in the total energy between wurtzite and zinc blende phases.[22,23] Our attempt to produce wurtzite InP using the same type of precursor, $\text{In}[\text{P}(t\text{-Bu})_2]_3$ instead of $\text{Ga}[\text{P}(t\text{-Bu})_2]_3$, and the same experimental condition as described by Cohen et al.[21] (presence of TAO/HDA (trioctylamine/hexyldecylamine) (1:2.5) solution at 330 °C for 72 h) did not succeed in forming wurtzite InP. Under these conditions, large tadpolelike zinc blende InP fibers with In spherules at the fiber tip were produced instead. We believe that indium metal formed by thermal decomposition is probably a better catalyst for growing anisotropic zinc blende InP crystallite than Ga metal.[4,11]

The thermal decomposition of $[(t\text{-Bu})_2\text{InP}(\text{SiMe}_3)_2]_2$ and $[\text{Cl}_2\text{InP}(\text{SiMe}_3)_2]_2$ precursors needs to be fast to facilitate the growth of small and straight nanorods. At a temperature of 170 °C, the reaction is completed in less than 30 min. If the reaction is too slow, then metallic indium can be covered with InP, and round particles are formed. We found that extremely small In particles easily oxidize in air, and In_2O_3 was detected by TEM. The presence of oxide can be detected in our samples by observing a shoulder at 470 nm in the absorption spectra and an emission peak at about 500 nm. (The band gap of In_2O_3 is 2.6 eV.) The morphology of the InP rods depends on the reaction time, temperature, nature of the stabilizer, and amount of In present during InP growth.

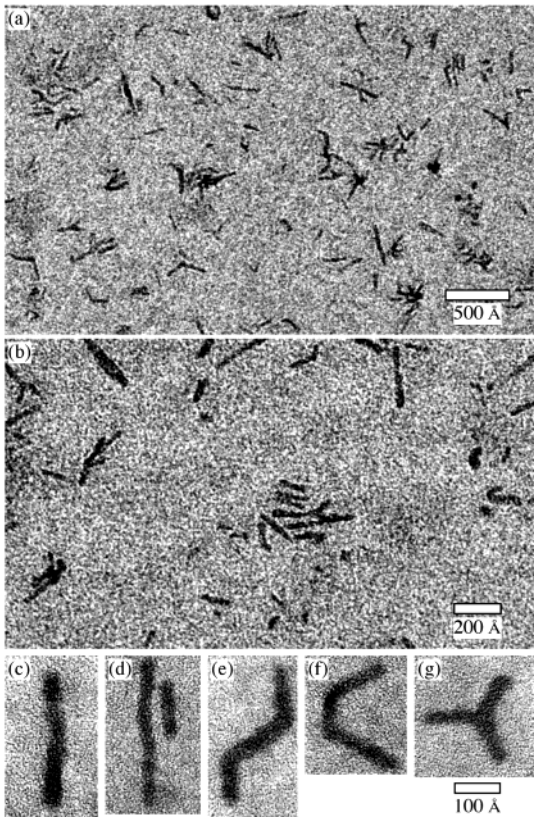

Figure 3. TEM images showing (a, b) ensemble of very small InP nanorods of about 30 Å diameter prepared from $[(t\text{-Bu})_2\text{InP-}(SiMe_3)_2]_2$ and $[Cl_2InP(SiMe_3)_2]_2$ precursors in TOA/DDA heated at 250 °C for 3 h. Typical configurations and shapes of these very small nanorods are shown: (c) a single rod, (d) parallel rods, (e) zigzag rod, (f) "U"-shaped rod, and (g) three-armed rod.

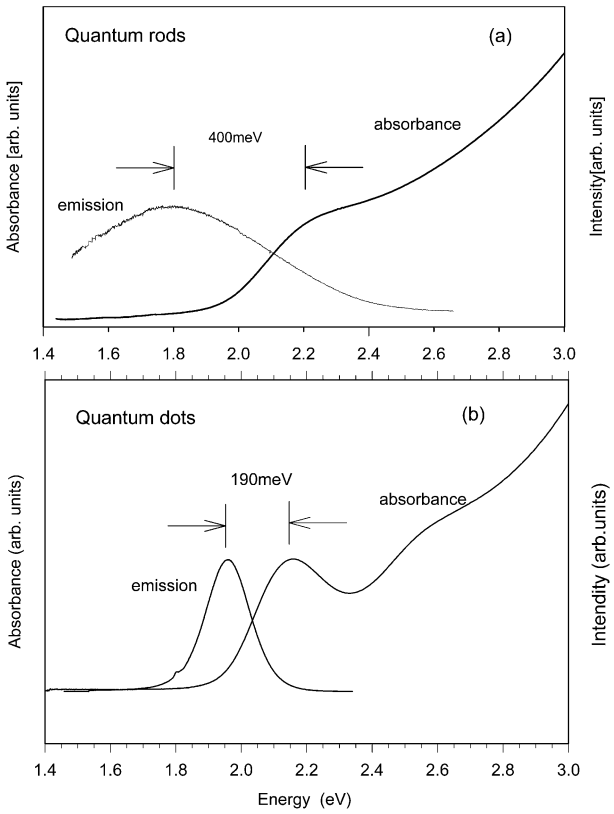

Figure 4. Absorption spectra for (a) InP quantum rods and (b) InP quantum dots (diameter ≈ 30 Å).

Metal indium particles that are associated with the InP rods need to be removed from the system after synthesis because they can accept charge and change the physical properties of the rods. We found that after synthesis the remaining In spherules can be partially removed by washing the sample with HF (0.5%) and extracted by forming an alloy with mercury added to the system.

Very small InP nanorods were also produced, with diameters of approximately 30 Å and lengths of up to about 330 Å (Figure 3). The presence of In and P in a ratio of 1:1 in these small nanorods was confirmed qualitatively using EDX, which also revealed oxygen in the samples. However, lattice fringes arising from the zinc blende structure of bulk InP were not detected. Instead, weak fringes with a spacing of 2.7 Å appeared in some regions, probably resulting from residual indium metal or a surface oxide layer. This behavior is similar to that of small InP quantum dots that also show weak crystallinity and the formation of oxide layers on the surface.[24]

Ensembles of very small nanorods show a variety of configurations. Straight nanorods often form small clusters with parallel (side-by-side) alignment, although the degree of ordering in these samples is relatively weak. A portion of the InP products also shows distorted shapes including zigzag, bent "U" or "V" shapes, or extension in multiple directions, forming spokes.

Quantum rods with diameters of 30−60 Å are soluble as colloidals and form a transparent colloidal solution. Absorption and emission spectra are in the visible spectral region, indicating that the nanorods are in the strong confinement regime. Quantum rods result when the nanorod diameter is reduced below the excitonic Bohr diameter, which is about 200 Å for InP. For quantum rods, the diameter and length determine the position of excitonic peaks. Quantum rods are in the transitional region between 0-D quantum dots and 1-D quantum wires and, as expected, strongly modify the electronic spectra[7] and the interparticle electronic interaction.[8,9] At a larger aspect ratio above 10, rods can be treated as 1-D quantum wires in which electrons and holes are bound into 1-D excitons. In Figure 3, we compare the absorption and emission spectra for quantum rods that have 28 ± 7 Å diameters and a broad length distribution from 100 to 300 Å with those for spherical InP QDs that were described in previous work[25] and that have roughly 32 ± 2.4 Å diameters. The red shift between the absorbing and emitting states is much larger for 1-D rods than for spherical QDs with roughly the same diameter. This behavior has been noted previously in the CdSe system.[7] For InP quantum rods, the absorption and emission spectra (Figure 4) have a broad band indicating a wide distribution in diameter. A narrower size distribution is needed for more precise studies of the red shift of emitting states with respect to absorbing states for InP rods.

The ability to generate nanorods and nanowires with sufficiently small diameters to exhibit strong quantum confinement offers numerous possibilities for optoelectronic devices. Here we have shown the ability to control the size

of InP nanorods down to the strongly confined quantum regime. The physical characteristics and optical signatures of these quantum rods will continue to be explored.

Acknowledgment. This work was supported by the U.S. Department of Energy, Office of Science, Office of Basic Energy Sciences, Division of Chemical Sciences, Geosciences and Biosciences.

References

(1) Gudiksen, M. S.; Lieber, C. M. *J. Am. Chem. Soc.* **2000**, *122*, 8801.
(2) Romanov, S. G.; Sotomayor Torres, C. M.; Yates, H. M.; Pemble, M. E.; Butko, V.; Tretijakov, V. *J. Appl. Phys.* **1997**, *82*, 380.
(3) Tang, C.; Fan, S.; Lamy de la Chapelle, M.; Dang, H.; Li, P. *Adv. Mater.* **2000**, *12*, 1346.
(4) Trentler, T. J.; Goel, S. C.; Hickman, K. M.; Viano, A. M.; Chiang, M. Y.; Beatty, A. M.; Gibbons, P. C.; Buhro, W. E. *J. Am. Chem. Soc.* **1997**, *119*, 2172.
(5) Peng, X.; Manna, L.; Yang, W.; Wickham, J.; Scher, E.; Kadavanich, A.; Alivisatos, A. P. *Nature* **2000**, *404*, 59.
(6) Tang, Z.; Kotov, N. A.; Giersig, M. *Science* **2002**, *297*, 237.
(7) Hu, J.; Li, L.; Yang, W.; Manna, L.; Wang, L.; Alivisatos, A. P. *Science* **2001**, *292*, 2063.
(8) Htoon, H.; Hollingsworth, J. A.; Malko, A. V.; Achermann, M.; Petruska, M. A.; Klimov, V. I. MRS Fall Meeting, Boston, MA, December 2−6, 2002.
(9) Kazes, M.; Lewis, D. Y.; Ebenstein, Y.; Mokari, T.; Banin, U. *Adv. Mater.* **2002**, *14*, 317.
(10) Huynh, W. U.; Dittmer, J. J.; Alivisatos, A. P. *Science* **2002**, *295*, 2425.
(11) Trentler, T. J.; Hickman, K. M.; Goel, S. C.; Viano, A. M.; Gibbons, P. C.; Buhro, W. H. *Science* **1995**, *270*, 1791.
(12) Yan, P.; Xie, Y.; Wang, W.; Liu, F.; Qian, Y. *J. Mater. Chem.* **1999**, *9*, 1833.
(13) Buhro, W. E. ACS Rocky Mountain Meeting, Albuquerque, NM, October 12−14, 2002.
(14) Gudiksen, M. S.; Wang, J.; Lieber, C. M. *J. Phys. Chem. B* **2001**, *105*, 4062.
(15) Duan, X.; Lieber, C. M. *Adv. Mater.* **2000**, *12*, 298.
(16) Bradley, D. C.; Frigo, D. M.; Hursthouse, M. B.; Hussain, B. *Organometallics* **1988**, *7*, 1112.
(17) Kan, S.; Mokari, T.; Rothenberg, E.; Banin, U. *Nat. Mater.* **2003**, *2*, 155.
(18) Nedeljkovic, J. M.; Micic, O. I.; Nozik, A. J., unpublished result.
(19) Soulantica, K.; Maisonnat, A.; Senocq, F.; Fromen, M.-C.; Casanove, M.-J.; Chaudret, B. *Angew. Chem., Int. Ed.* **2001**, *40*, 2984.
(20) Soulantica, K.; Maisonnat, A.; Fromen, M.-C.; Casanove, M.-J.; Lecante, P.; Chaudret, B. *Angew. Chem., Int. Ed.* **2001**, *40*, 448.
(21) Kim, Y.-H.; Jun, Y.-w.; Jun, B.-H.; Lee, S.-M.; Cheon, J. *J. Am. Chem. Soc.* **2002**, *124*, 13656.
(22) Yeh, C.-Y.; Lu, Z. W.; Froyen, S.; Zunger, A. *Phys. Rev. B* **1992**, *46*, 10086.
(23) Yeh, C.-Y.; Wei, S.-H.; Zunger, A. *Phys. Rev. B* **1994**, *50*, 2715.
(24) Mićić, O. I.; Ahrenkiel, S. P.; Nozik, A. J. *Appl. Phys. Lett.* **2001**, *78*, 4022.
(25) Mićić, O. I.; Jones, K. M.; Cahill, A.; Nozik, A. J. *J. Phys. Chem. B* **1998**, *102*, 9791.

NL034152E